Low-Temperature Growth of Nanocrystalline Mn-Doped ZnS Thin Films Prepared by Chemical Bath Deposition and Optical Properties

Alireza Goudarzi,[†] Ghaffar Motedayen Aval,[†] Sung Soo Park,[‡] Myeon-Cheon Choi,[‡] Reza Sahraei,[§] M. Habib Ullah,[‡] Armen Avane,[⊥] and Chang-Sik Ha*,[‡]

Department of Chemistry, Tarbiat Moallem University, 49 Mofateh Avenue, Tehran 15719-14911, Iran, National Research Laboratory of Nano-Information Materials, Department of Polymer Science and Engineering, Pusan National University, Busan 609-735, Republic of Korea, Department of Chemistry, University of Ilam, Ilam 69315-516, Iran, and Department of Chemistry, Maragheh University, Maragheh 55181-83111, Iran

Received December 10, 2008. Revised Manuscript Received April 11, 2009

ZnS:Mn thin films were deposited on quartz, Si (polycrystalline), and glass substrates using a chemical bath deposition (CBD) method in an aqueous solution containing ethylene diamine tetra acetic acid disodium salt (Na_2EDTA) as the complexing agent for zinc ions and thioacetamide (TAA) as the sulfide source at temperatures ranging from 50 to 80 °C. ZnS:Mn thin films with thicknesses ranging from 60 to 450 nm were synthesized at various Mn^{2+}/Zn^{2+} molar ratios ranging from 1 to 4. The effects of the process parameters on the properties of ZnS:Mn films were investigated. The films were characterized by energy-dispersive X-ray spectrometer (EDX), inductively coupled plasma atomic emission spectroscopy (ICP-AES), Rutherford backscattering (RBS), secondary ion mass spectrometry (SIMS), attenuated total reflection-Fourier transform infrared (ATR-FTIR) spectroscopy, X-ray photoelectron spectroscopy (XPS), X-ray diffractometer (XRD), high-resolution transmission electron microscopy (HRTEM), field emission scanning electron microscopy (FE-SEM), ultraviolet -visible light (UV−vis) spectroscopy, and photoluminescence (PL) spectroscopy. The results showed that the deposition time, temperature, and Mn doping concentration can affect the composition, surface morphology, crystallinity, thickness, grain size, and hence, the photoluminescence and transmission spectra of the films. UV−vis transmission spectroscopy showed that the prepared films were highly transparent (>80%) in the visible region. X-ray diffraction showed that the films consisted of small ZnS:Mn nanocrystallites, 3.0−4.7 nm in size, showing quantum size effects. FE-SEM revealed a homogeneous morphology, dense nanostructures, and a narrow grain size distribution.

Introduction

There has been increasing interest in the development of reliable luminescent materials for applications in flat panel displays. Most research efforts in this area have been directed toward film deposition techniques and different types of materials and dopants that are used as active components in electroluminescent devices.

Zinc sulfide is a semiconductor suitable for use as a host matrix for a wide variety of dopants on account of its wide energy band gap. The luminescence properties of this material doped with Mn have proven to be suitable for electroluminescence applications.[1−3] Manganese is generally incorporated as Mn^{2+} ion in the substitutional sites of the ZnS lattice. The excitation and decay of this ion produces a yellow luminescence at approximately 590 nm, which is associated with a transition between the $^4T_1$ and $^6A_1$ energy levels.[4] The $^4T_1 \rightarrow {}^6A_1$ Mn^{2+} emission intensity generally increases with increasing Mn^{2+} concentration. However, the quenching of Mn^{2+} emission has been observed at high Mn^{2+} concentrations.[5,6]

The techniques used to deposit ZnS films have different natures. Among them, the most common are sputtering,[7] sol−gel,[1,8] spray pyrolysis,[9,10] chemical vapor deposition (CVD),[11,12] molecular beam epitaxy,[13] atomic layer epitaxy (ALE),[14] and chemical bath deposition (CBD).[15−21]

* Corresponding author. E-mail: csha@pusan.ac.kr. Tel.: 82-51-510-2407. Fax: 82-51-514-4331.
[†] Tarbiat Moallem University.
[‡] Pusan National University.
[§] University of Ilam.
[⊥] Maragheh University.

(1) Tang, W.; Cameron, D. C. *Thin solid Film* **1996**, *280*, 221.
(2) Yang, H.; Holloway, P. H. *J. Phys. Chem. B* **2003**, *107*, 9705.
(3) Leeb, J.; Gebhardt, V.; Muller, G.; Haarer, D.; Su, D.; Giersig, M.; McMahon, G.; Spanhel, L. *J. Phys. Chem.B* **1999**, *103*, 7839.
(4) Bhargava, R. N.; Gallagher, D.; Hong, X.; Nurmikko, A. *Phys. Rev. Lett.* **1994**, *72*, 416.
(5) Khosravi, A. A.; Kundu, M.; Jatwa, L.; Deshpande, S. K.; Bhagwat, U. A.; Sastry, M.; Kulkarni, S. K. *Appl. Phys. Lett.* **1995**, *67*, 2702.
(6) Borse, P. H.; Srinivas, D.; Shinde, R. F.; Date, S. K.; Vogel, W.; Kulkarni, S. K. *Phys. Rev. B* **1999**, *60*, 8659.
(7) Le-Xi, S.; Kuen-Huei, C.; Huey-Liang, H. *Appl. Surf. Sci.* **2003**, *212*, 305.
(8) Nina, I. K.; Eugenia, V. B.; Chad, C. W.; Benjamin, R. M.; Thomas, M. *Chem. Mater.* **2000**, *12*, 383.
(9) López, M. C.; Espinos, J. P.; Martín, F.; Leinen, D.; Ramos-Barrado, J. R. *J. Cryst. Growth* **2005**, *285*, 66.
(10) Hernández-Fenollosa, M. A.; López, M. C.; Donderis, V.; González, M.; Marí, B.; Ramos-Barrado, J. R. *Thin Solid Films* **2008**, *516*, 1622.
(11) Lee, E. Y. M.; Tran, N. H.; Russell, J. J.; Lamb, R. N. *J. Phys. Chem. B* **2003**, *107*, 5208.
(12) Chun, J.; Talaga, D. S.; Zink, J. I. *J. Am. Chem. Soc.* **1997**, *119*, 163.
(13) Zhang, L.; Szargan, R.; Chassé, T. *Appl. Surf. Sci.* **2004**, *227*, 261.

10.1021/cm803329w CCC: $40.75
Published on Web 05/06/2009

Table 1. Concentrarions and Molar Ratios of Main Species in Precursor Solutions

species	Zn^{2+}	Mn^{2+}	TAA	Na_2EDTA	$NH_4(CH_3COO)$
conc. (mol/L)	0.0006	0.0006−0.0024	0.0012	0.0003	0.002
molar ratio (relative to Zn^{2+})	1	1−4	2	0.5	3.3

Table 2. Changes in the Parameters of the ZnS:Mn Thin Films Prepared at 80 °C from Precursor Solutions with a Mn^{2+}/Zn^{2+} Molar Ratio of 4

deposition time (h)	thickness (Å)	band gap (eV)	excitation peak (nm)	intensity (arb. unit)	grain size (nm)	S/Zn (at ratio)	Mn/Zn (at %)
4	1941	3.75	329.1	70	3.3	0.96	0.44
6	2582	3.68	330.6	115	3.46	0.96	0.50
8	3268	3.68	335.8	164	4.0	0.95	0.61
10	3821	3.67	340.0	229[a]	4.16	0.94	0.94
12	4350	3.66	340.8	88	4.6	0.93	1.25
15	4525	3.65	343.8	40	4.7	0.92	1.55

[a] After 10 h, the quenching effect appeared.

CBD is widely used for film deposition in photovoltaic applications. Chemical bath deposition of ZnS thin films has been carried out usually in an alkaline ammonia or hydrazine precursor solution by many researches,[16−19] whereas species such as $Zn(OH)_2$ and/or ZnO are present in their films.[19−21] In this work, a pH of 6.0 in the precursor solution is chosen to avoid the formation of such undesired species in the films. Although the CBD has been used for the preparation of doped metal sulfides,[22,23] there are no reports on ZnS:Mn thin film preparations using this method in an ammonia/hydrazine-free media (environment). The CBD method is simple, convenient, and cost-effective because it is normally carried out at atmospheric pressure (usually air) and near ambient temperatures.[24] It has the advantage of not requiring vacuum systems and is compatible with large area deposition.[25]

This paper reports for the first time the preparation of Mn^{2+} doped ZnS thin films by CBD method at different temperatures and Mn^{2+} concentrations at pH of 6.0. The effect of the deposition temperature, deposition time, and doping level on composition, nanostructure, surface morphology, and optical properties of ZnS:Mn films are examined.

Experimental Section

Preparation of Mn^{2+}-Doped ZnS Thin Films. All chemicals were purchased from Sigma-Aldrich Company and used without further purification. Nanocrystalline ZnS:Mn thin films were deposited on quartz, polycrystalline Si, and commercial microscope slide glass substrates using Na_2EDTA solution as a complexing agent for zinc ions. The chemical bath solution was prepared as follows: 6 mL of a 1 M (M = mol/L) zinc acetate [$Zn(CH_3COO)_2 \cdot 2H_2O$] solution, 15 mL of a 0.2 M Na_2EDTA solution, and 20 mL of a 1 M ammonium acetate [$CH_3COONH_4 \cdot 2H_2O$] were mixed. One molar manganese acetate [Mn $(CH_3COO)_2 \cdot 2H_2O$] solution was then added in desired amounts. The Mn^{2+} to Zn^{2+} molar ratio in the precursor solution was varied from 1 to 4. In the next step, 30 mL of a 0.4 M thioacetamide (TAA) [CH_3CSNH_2] solution was added and the pH was adjusted to 6.0 by adding a 1 M NaOH solution. Finally, deionized water was added to the solution to make the volume close to 100 mL and pH was adjusted to 6.0 again and then the volume was increased to 100 mL by adding a few drops of deionized water. Different baths were prepared using these solutions, and deposition was carried out at different temperatures ranging from 50 to 80 °C for a duration ranging from 4 to 15 h. The amounts of the main species in the bath solution in terms of mol/L and molar ratios are given in Table 1.

Before film deposition, the substrates were placed in 4% HF solution for 10 min to obtain a rough surface and were cleaned ultrasonically sequentially in acetone, 2-propanol, and deionized water. The substrates were then dried for one hour in an oven at 90 °C. At the same time, six of these glass substrates were inserted vertically into the reaction container, which was then placed in a thermostat bath set to the desired temperature. The chemical bath solution was not stirred during the film deposition. The coated substrates were removed at the end of deposition, washed in deionized water, dried in air at room temperature, and then characterized. Both sides of the glass substrates were coated with the films. For the optical transmittance measurements, the coating on one side of the substrates was removed by cotton swabs moistened with dilute HCl.

Characterization of Thin Films. The atomic composition of the films was analyzed by energy-dispersive X-ray spectrometer (EDX) using an Oxford INCA II energy solid state detector. Inductively coupled plasma atomic emission spectroscopy (ICP-AES; Varian Vista-Pro) was employed to determine the elemental content of the ZnS:Mn thin films. The chemical composition of the thin films was also determined by Rutherford backscattering (RBS) measurements. For RBS measurements, 2.3 MeV He^+ ions were used as incident ions and the backscattered particles were detected by a silicon surface barrier detector at a 165° scattering angle relative to the incident beam. Secondary ion mass spectrometry (SIMS) was used to determine the distribution of the elements in ZnS:Mn films. All analyses were performed using a CAMECA IMS-6f Magnetic Sector SIMS. To investigate the presence of

(14) Tsukasa, T.; Atsushi, O.; Susumu, K.; Hidehiro, Y.; Hirotaro, M.; Hiroshi, Y. *Langmuir* **2000**, *16*, 5820.
(15) Goudarzi, A.; Motedayen Aval, G.; Sahraei, R.; Ahmadpoor, H. *Thin Solid Films* **2008**, *516*, 4953.
(16) Oladeji, I. O.; Chow, L. *Thin Solid Films* **1999**, *339*, 148.
(17) Hubert, C.; Naghavi, N.; Canava, B.; Etcheberry, A.; Lincot, D. *Thin Solid Films* **2007**, *515*, 6032.
(18) Ben Nasr, T.; Kamoun, N.; Kanzari, M.; Bennaceur, R. *Thin Solid Films* **2006**, *500*, 4.
(19) Oladeji, I. O.; Chow, L. *Thin Solid Films* **2005**, *474*, 77.
(20) Gode, F.; Gumus, C.; Zor, M. *J. Cryst. Growth* **2007**, *299*, 136.
(21) Hubert, C.; Naghavi, N.; Etcheberry, A.; Roussel, O.; Hariskos, D.; Powalla, M.; Kerrec, O.; Lincot, D. *Phys. Status Solidi A* **2008**, *205*, 2335.
(22) Altosaar, M.; K. Ernits, K.; Krustok, J.; Varema, T.; Raudoja, J.; Mellikov, E. *Thin Solid Films* **2005**, *480−481*, 147.
(23) Portillo-Moreno, O.; Lima-Lima, H.; Ramirez-Falcon, V.; Martinez-Juarez, J.; Juarez-Diaz, G.; Lozada-Morales, R.; Rebollo-Plata, B.; Palomino-Merino, R.; Soto, A. B.; Zelaya-Angel, O. *J. Electrochem. Soc.* **2006**, *153* (10), G 926.
(24) Hodes, G.; *Chemical Solution Deposition of Semiconductor Films*; Marcel Dekker Inc.: New York, 2003.
(25) Mane, R. S.; Lokhande, C. D. *Mater. Chem. Phys.* **2000**, *65*, 1.

organic and/or other compounds in films, the attenuated total reflection-Fourier transform infrared (ATR-FTIR) spectrum was obtained by a BRUKER EQUINOX 55 spectrometer in the range of 200−6000 cm^{-1} with a resolution of 0.5 cm^{-1}. X-ray photoelectron spectroscopy (XPS) measurements were performed to investigate the surface composition of the ZnS:Mn thin films by a Lebold EA 11 MCD spectrometer with a hemispherical electron analyzer and an Mg Kα X-ray source ($h\nu$ = 1253.6 eV) with a beam of 1 mm in diameter.

The surface morphology of the ZnS:Mn films were observed by field emission scanning electron microscopy (FE-SEM; Hitachi S-4200) under an acceleration voltage of 15 kV at the Busan Center of the Korea Basic Science Institute (KBSI Busan).

The crystallinity, phase, and orientation of the ZnS:Mn films were determined by X-ray diffraction (XRD) using a Rigaku Mini flex X-ray diffractometer with a Cu Kα radiation source (λ = 0.15406 nm) at 40 kV and 30 mA. The films were scanned in the range of 2θ = 20−60°. Transmission electron microscopy (TEM) images were obtained using a JEOL-JEM 2010 electron microscope at an acceleration voltage of 200 kV. For high-resolution TEM (HRTEM) measurements, ZnS:Mn thin film was scrapped from the substrate and then poured into ethanol, forming a very dilute colloidal solution and used for the measurement.

The photoluminescence emission and excitation spectra of the films were measured using a Hitachi F-4500 fluorescence spectrophotometer. A xenon lamp was used for excitation of the ZnS:Mn films in the UV region (see the Supporting Information, Table S-1). The UV−vis spectra were obtained using a Hitachi U-2010 spectrophotometer. The film thickness was determined using an α-step profilometer (Dektak^3, Veeco Inst.). All measurements were carried out at room temperature.

Results and Discussion

Compositional, Structural, and Morphological Characterization. Chemical composition of deposited ZnS:Mn thin films on polycrystalline silicon were analyzed by EDX, ICP-AES, RBS, SIMS, ATR-FTIR, and XPS. EDX analysis indicated the presence of zinc, sulfur and oxygen for all deposited films (Figure S-1 in the Supporting Information). The obtained Zn/S atomic ratios were listed in Table 2. The oxygen peak was also observed in the EDX data of the polycrystalline silicon substrate. (For reference, the EDX data for the polycrystalline silicon substrate are given in the Supporting Information, Figure S-2 and Table S-2.) As seen in Table 2, although some S vacancy is observed in all films, the S/Zn atomic ratios are almost close to their stoichiometry.

As the percentage of manganese in films was less than the detection limit of EDX, however, the Mn concentration in ZnS:Mn films was determined by ICP-AES measurements. The obtained Mn/Zn atomic percent ratios in ZnS:Mn films prepared from a precursor solution with Mn/Zn molar ratio of 4 at 80 °C and different deposition times were listed also in Table 2. As seen from Table 2, with increasing the deposition time, Mn/Zn atomic ratios in films increase, though these values are all much less than one-two hundredth of initial Mn concentration in the precursor solution. This large difference is attributed to the large difference in the solubility products of ZnS (1.1×10^{-24}) and MnS (1.0×10^{-13}), which makes the codeposition of ZnS and MnS quite difficult. EDTA was used as a complexing agent to coordinate with Zn^{2+} ions. Because the formation constant of

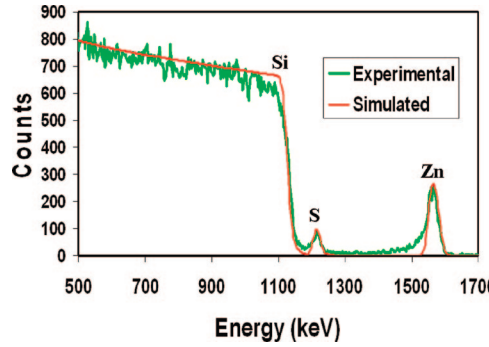

Figure 1. RBS spectrum of the ZnS:Mn thin film deposited on silicon substrate at 80 °C for 10 h.

ZnEDTA (3.2×10^{16}) is much higher than that of MnEDTA (6.2×10^{13}), ZnEDTA is formed as a major complex. It is important to note that in precursor solutions without using EDTA, the obtained films did not show any Mn characteristic emission (at 590 nm) regardless of different Mn/Zn molar ratios, which means that Mn ions could not be doped with ZnS to form ZnS:Mn films in the absence of EDTA. The highest concentration of Mn doped into nanocrystalline ZnS thin films is found to be 1.5% (relative to Zn^{2+}). Optical properties of ZnS:Mn films will be discussed later.

Figure 1 shows the typical RBS spectrum of the ZnS:Mn thin film deposited on a silicon substrate at 80 °C for 10 h. The integrated number of counts under Zn and S curves (peak and tail) agrees well with the number of counts under the simulated peaks, from which the composition in the ZnS:Mn thin film can be estimated as Zn/S = 1:0.95. The very low Mn concentration in the films could not be detected by RBS analysis. Oxygen has been detected in many chemical bath deposited thin films,[19−21] probably because of the chemical composition of their precursor solutions. The absence of oxygen peak in the RBS spectrum indicates, however, the absence or very low concentration, if any, of impurities such as $Zn(OH)_2$ or ZnO in the film for this work.

To investigate the presence of organic and/or other compounds such as $Zn(OH)_2$ and ZnO as impurities in the ZnS:Mn thin films, we obtained the attenuated total reflection-Fourier transform infrared (ATR-FTIR) spectrum in transmittance mode of a ZnS:Mn thin film on a quartz substrate. Literatures reported the existence of isothiocyanate groups (−N═C═S), Zn−O, or Zn−OH bonds, and adsorbed H_2O in CBD-ZnS thin films.[26−28] Zn−OH stretching and bending mode is seen at 1115 and 648 cm^{-1}, respectively,[29,30] Zn−O in ZnO powder is observed at 430 cm^{-1};[31] isothiocyanates (−N═C═S) have a strong peak in the 2000−2273 cm^{-1} domain;[34] whereas Zn−S in the pure ZnS powder is

(26) Nakada, T.; Furumi, K.; Mizutani, M.; Hagiwara, Y.; Kunioka, A. *Technical Digest of the 11th International Photovoltaic Science and Engineering Conference*, Hokkaido, Japan, Sept 20−24, 1999; p 81.
(27) Mokili, B.; Charreire, Y.; Cortes, R.; Lincot, D. *Thin Solid Films* **1996**, *288*, 21.
(28) El Maliki, H.; Bernede, J. C.; Marsillac, S.; Pinel, J.; Castel, X. Pouzet. *J. Appl. Surf. Sci.* **2003**, *205*, 65.
(29) Wegmuller, F. *J. Colloid Interface Sci.* **1987**, *116*, 312.
(30) Kauffman, J. W.; Hauge, R. H.; Margrave, J. L. *J. Phys. Chem.* **1985**, *89*, 3541.
(31) Ferraro, J. R. *Low-Frequency Vibrations of Inorganic and Coordination Compounds*; Plenum: New York, 1971.
(32) Socrates, G. *Infrared Raman Characteristic Group Frequencies*; Wiley: New York, 2001.

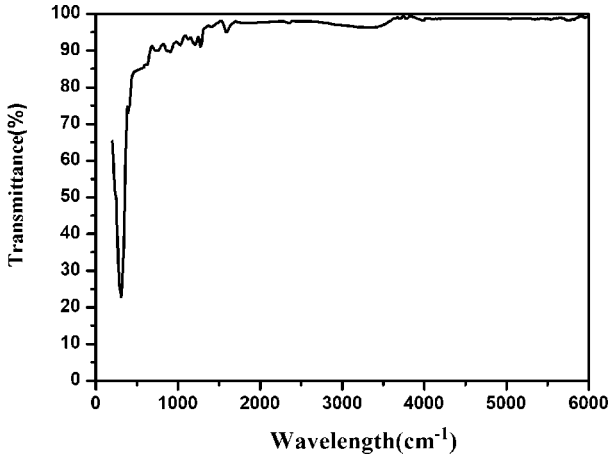

Figure 2. ATR-FTIR transmittance spectrum of the ZnS:Mn thin film deposited on quartz substrate at 80 °C for 10 h.

detected as a strong peak at 298 cm^{-1}.[31] In Figure 2, the ATR-FTIR spectrum of one of the ZnS:Mn thin films in this work, besides the Zn−S peak at 298 cm^{-1}, no other peaks due to impurities are observed except for a very weak peak at 1600 cm^{-1} and a broad weak peak at 3200−3500 cm^{-1} that must be related to the stretching and bending modes of trace amounts of adsorbed water on the film.

Surface analyses based on XPS were carried out to acquire chemical bonding information for the CBD ZnS:Mn thin films. The investigations were particularly aimed at characterizing the film coverage and, most importantly, determining whether ZnS:Mn thin films contained $Zn(OH)_2$ and ZnO as reported by other researchers who fabricated ZnS thin films by chemical bath deposition.[19−21] Figure 3a shows an XPS survey spectrum of the ZnS:Mn thin film deposited on the polycrystalline silicon substrate at 80 °C for 10 h. The dominant peaks for Zn, S, and O 1s and C 1s peaks hint that a uniform film is formed, since no substrate peaks such as Si, In, or Sn are visible. The carbon peak must be mainly due to surface contamination. The low Mn concentration on the surface of the film was not detected also by XPS analysis.

To reveal the type of chemical bonds of oxygen in the film, a high resolution O 1s spectrum was recorded for the ZnS:Mn thin film deposited on Si substrate at 80 °C, shown in Figure 3b. The binding energies related to different species assigned as the following: 530 to 530.8 eV for oxides, 531.5 to 532 eV for hydroxides and 533 to 534 eV for H_2O.[33,34] Therefore, the observed peak at 533.5 eV, is assigned to H_2O. Figure 3c displays the Zn $^2P_{3/2}$ core level spectrum of the ZnS:Mn thin film deposited on the Si substrate at 80 °C. By fitting with component Gaussian curves, the observed peak at 1021 eV was assigned to the ZnS.[35]

Secondary ion mass spectrometry (SIMS) was used to determine the distribution of elements in the films. Besides, because of its high sensitivity to trace amounts of elements, SIMS was used to detect the presence or absences of Mn on

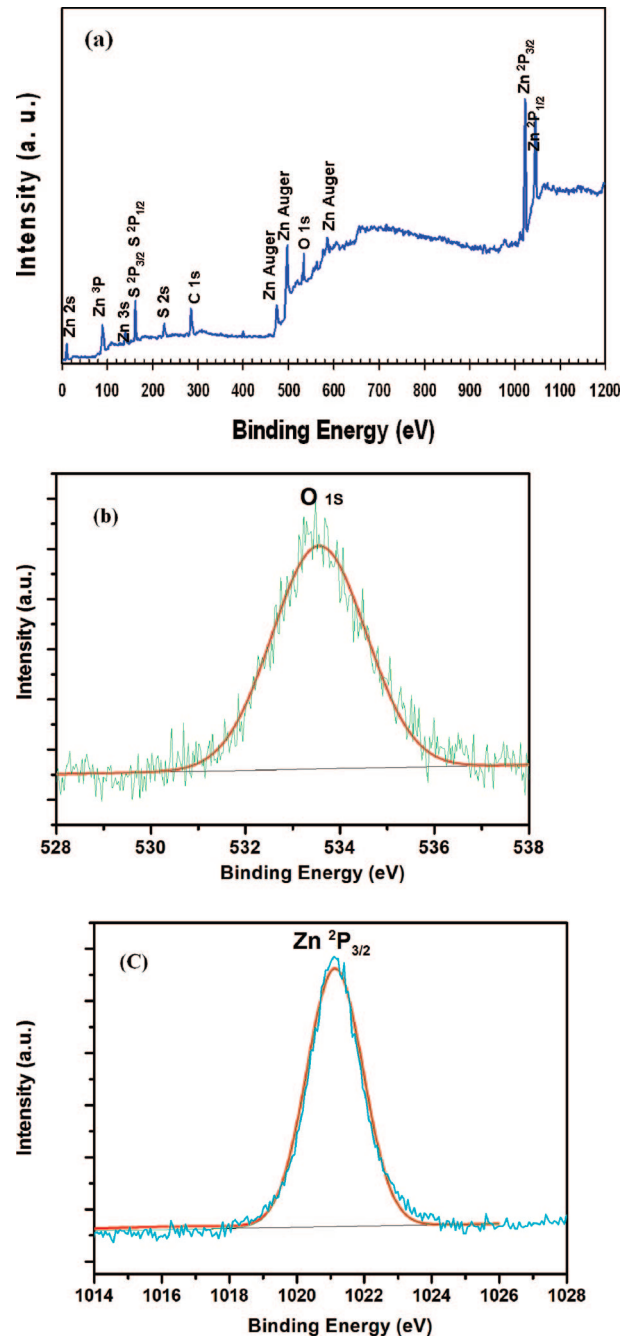

Figure 3. (a) XPS survey spectrum as well as high-resolution (b) O1s and (c) Zn $^2P_{3/2}$ spectra of the ZnS:Mn thin film deposited on a polycrystalline silicon substrate at 80 °C for 10 h.

or near the surface of the film. Figure 4 shows the result of SIMS depth profile on the ZnS:Mn thin film deposited on a silicon substrate from a precursor solution with Mn/Zn molar ratio of 4 at 80 °C for 10 h. All expected elements of interest are found to be homogeneously distributed across the entire film, which confirms the homogeneous formation of ZnS:Mn thin film on the substrate. The SIMS analysis also shows the presence of Mn on the surface of the films, despite the fact that the XPS analysis could not detect any Mn on the surface of the films because of very low concentration of Mn in the films and on its surface. The detected minor amount of oxygen is not surprising and is related to adsorbed

(33) Eisele, W.; Ennaoui, A.; Schubert-Bischoff, P.; Giersig, M.; Pettenkofer, J.; Krauser, J.; Lux-Steiner, M.; Zweigart, C.; Karg, F. *Sol. Energy Mater. Sol. Cells* **2003**, *75*, 17.
(34) Bayon, R.; Maffiotte, C.; Herrero, J. *Thin Solid Films* **1999**, *353*, 100.
(35) Makhova, L. V.; Konovalov, I.; Szargan, R.; Aschkenov, N.; Schubert, M.; Chasse, T. *Phys. Status Solidi C* **2005**, *2*, 1206.

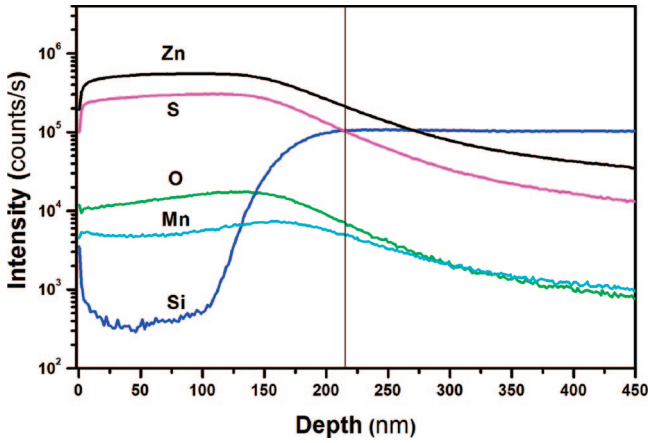

Figure 4. SIMS depth profile data of the ZnS:Mn thin film prepared from the precursor solution of Mn/Zn = 4 at 80 °C for 10 h.

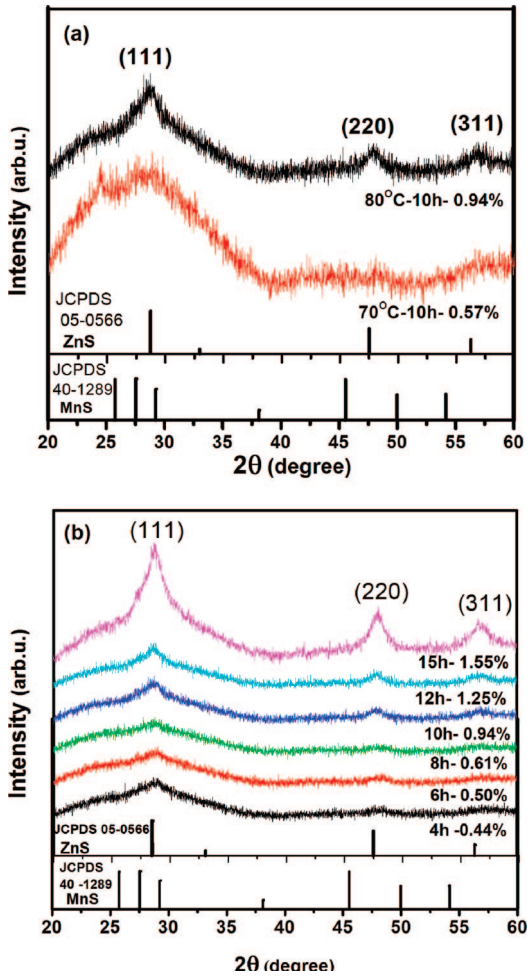

Figure 5. XRD patterns of ZnS:Mn films deposited at (a) different temperatures for 10 h, and (b) different deposition times at 80 °C. The % number in this figure denotes the Mn/Zn at %, as listed in Table 2.

water on the film. As mentioned before, the XPS and ATR-FTIR analyses also confirmed the presence of water in the films.

Figure 5a shows XRD patterns of ZnS:Mn films deposited on glass substrates at 70 and 80 °C for 10 h. Figure 5b shows XRD patterns of ZnS:Mn films with different Mn concentration (relative to Zn) prepared in different deposition times from 4 to 15 h at 80 °C. The diffraction peaks at 28.5, 47.5,

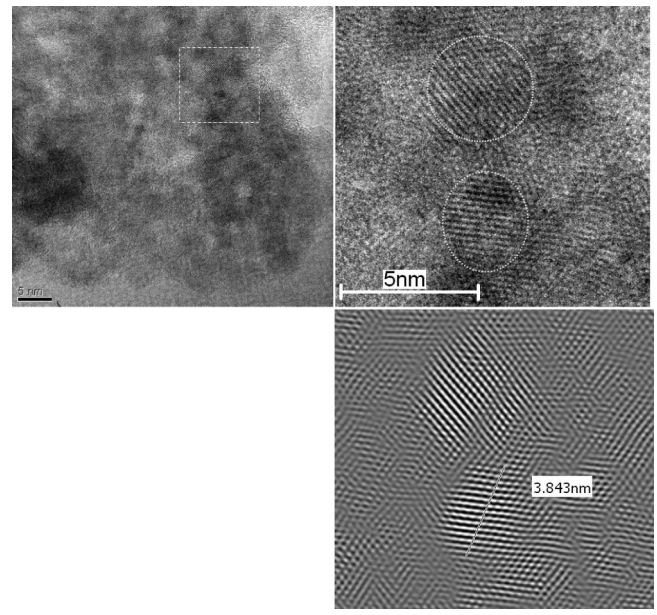

Figure 6. TEM image of the ZnS:Mn thin film prepared at 80 °C during 10 h deposition, (top left), and HRTEM images of selected area (top right and bottom).

and 56.3° were assigned to the (111), (220), and (311) planes of the cubic zinc blend structure (JCPDS No.05 −0566), as denoted by the vertical lines in panels a and b in Figure 5. XRD patterns revealed the films to be polycrystalline. There were no obvious structural phase differences in XRD results of the Mn-doped ZnS films with different Mn concentrations.

For all samples, the XRD peaks were quite broad, indicating nanosize particles. On the basis of the full width at half-maximum of (111) peak and applying the Debeye−Scherrer equation,[15] the average nanocrystallite size in the ZnS:Mn films was estimated to be 3.0 and 4.2 nm at 70 and 80 °C, respectively. Figure 6 shows a TEM image of the ZnS:Mn film prepared at 80 °C, which supports the nanocrystallite size estimated from the XRD data.

The broad hump at 2θ of approximately 25° was attributed to the amorphous nature of the glass substrate. As shown in panels a and b in Figure 5, the intensities of the peaks increase and become narrower with increasing temperature or deposition time, indicating an improvement in crystallinity and an increase in nanocrystallite size.

Figure 7 and Table 2 show the dependence of the nanocrystallite size and film thickness as a function of the deposition times for the ZnS:Mn films prepared at 80 °C. The nanocrystallite size was estimated using the Debye−Scherrer formula. The nanocrystallite size decreased from 4.7 to 3.3 nm when the deposition time was decreased from 15 to 4 h. Therefore, the nanocrystalline ZnS:Mn films are expected to be in the strong confinement regime considering that the excitonic diameter of ZnS is approximately 5 nm.[12] The increasing band gap energy of the films with decreasing deposition time (Table 2) supports the decrease in nanocrystallite size and confirms the quantum confinement effects in the films.

Morphological Characterization. The growth rate of the film is one of the deposition parameters that influence the surface morphology and grain geometry in thin polycrystalline films. In the CBD technique, the growth rate increases

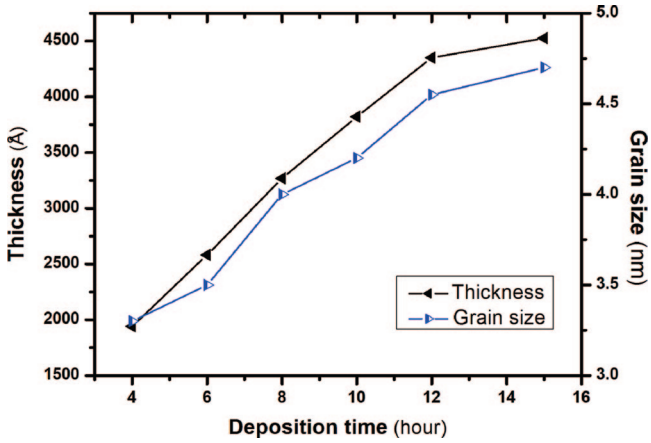

Figure 7. Change in film thickness and grain size as a function of the deposition time at 80 °C with a Mn^{2+}/Zn^{2+} molar ratio of 4 in the precursor solution.

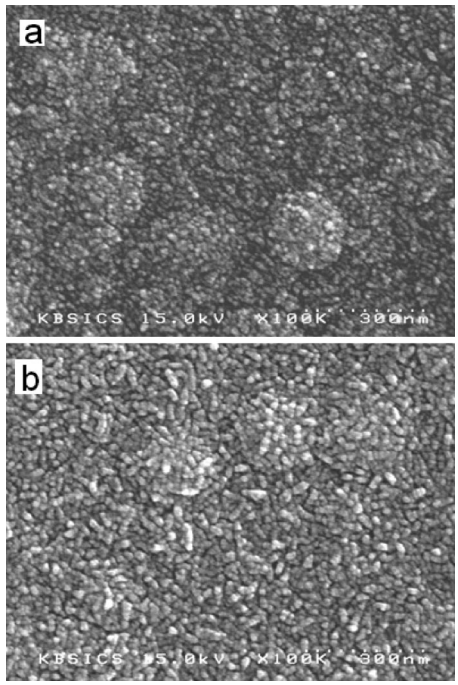

Figure 8. FE-SEM images of ZnS:Mn films prepared using a precursor solution with a Mn^{2+}/Zn^{2+} molar ratio of 4 at: (a) 70 and (b) 80 °C for 10 h. (Note: the bright dots on the grains are metals formed by sputtering during FE-SEM sample preparation.)

with increasing temperature and reactant concentration. The film surface was examined by FE-SEM. The ZnS:Mn films showed a surface structure consisting of grains with different sizes and morphologies depending on the deposition temperature. Images a and b in Figure 8 show SEM images of the films deposited at 70 and 80 °C for 10 h (the optimum deposition time and temperatures). At both temperatures, the film compactness was high, the surface's uniformity was good, the particle size was quite fine, and the particle size distribution was also narrow. These characteristics are in good agreement with the film's high transparency, which will be discussed in the next section. As shown in images a and b in Figure 8, the grains aggregated to form clusters. The size of the grains and clusters decreased and the surface roughness was improved with decreasing temperature. Images a and b in Figure 8 show that the average size of the observable features was approximately 10 and 20 nm, respectively, whereas the average nanocrystallite size estimated from the XRD peaks (Figure 5a) was 3.0 and 4.2 nm, respectively. This suggests that each feature in images a and b in Figure 8 is a polycrystallite grain.

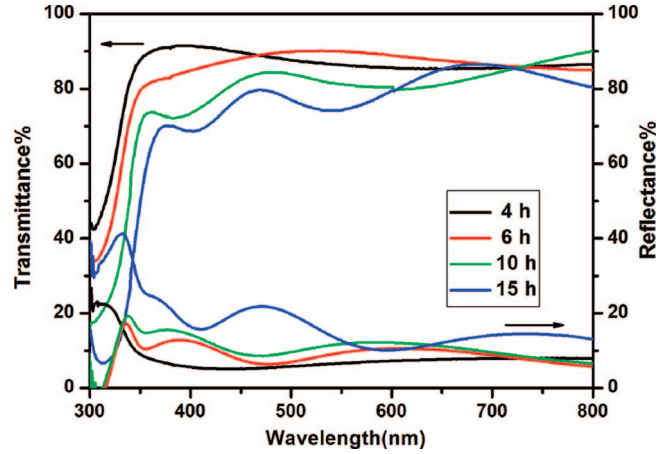

Figure 9. UV−visible transmission and reflection spectra of the prepared films from precursor solutions with a Mn^{2+}/Zn^{2+} molar ratio of 4 at 80 °C and at different deposition times.

Optical Properties. *UV Spectrophotometer Measurements.* Figure 9 shows the transmission and reflection spectra of the ZnS:Mn films grown on a glass substrate at 80 °C. This figure shows that the films are highly transparent in the visible region. The transmission for the films deposited for 10 h (Figure 9) was 85% between 420 and 800 nm, with a minimum of 80% at approximately 600 nm. The sharp absorption edge and high transmission values of the ZnS:Mn films at wavelengths >400 nm demonstrates a narrow grain size distribution as well as a low concentration of defects, such as pits and voids in the films.[36] This high-quality assignment was confirmed by FE-SEM images of the films (Figure 8b).

The optical absorption coefficients (α) were calculated using the following equation[37]

$$T = (1 - R)\exp(-\alpha t) \quad (1)$$

Where T is transmittance, R is reflectance, and t is the film thickness. The absorption coefficient (α) is related to the incident photon energy as follows

$$\alpha h\upsilon = k(h\upsilon - E_g)^{n/2} \quad (2)$$

where k is a constant, E_g is the separation between the valence and conduction bands (the energy gap), and n is a constant equal to 1 for direct band gap semiconductors and 4 for indirect band gap materials. A plot of $(h\alpha\upsilon)^2$ versus $h\upsilon$ (Figure 10) is linear at the absorption edge, which means that the mode of transition in these films has a direct nature. The band gap energy, E_g, can be obtained from an extrapolation of the straight-line portion of the $(h\alpha\upsilon)^2$ versus $h\upsilon$ plot to zero absorption coefficient value.[38] Table 2 lists the estimated band gap values.

(36) Ramamoorthy, K.; Sanjeeviraja, C.; Jayachandran, M.; Sankaranarayanan, K.; Bhattacharya, P.; Kukreja, L. M. *J. Cryst. Growth* **2001**, *226*, 281.
(37) Dakhel, A. A. *Phys. Status Soldi A* **2008**, *205*, 11–2704.

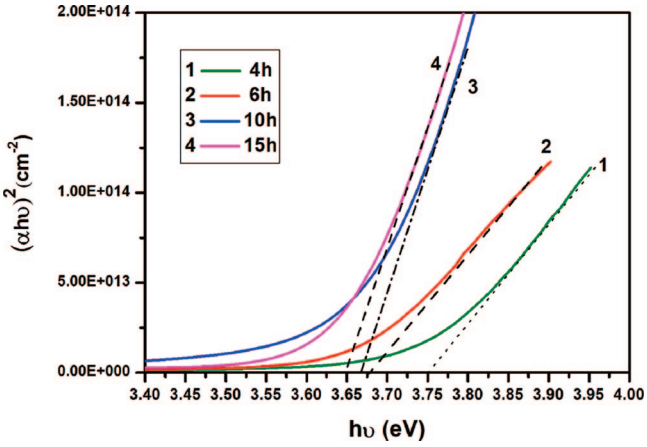

Figure 10. Plot of $(\alpha h\nu)^2$ for ZnS:Mn thin films as a function of the deposition time at 80 °C.

As shown in Figure 10 and Table 2, the band gap energy clearly shifts to a lower wavelength (higher energy) with decreasing deposition time. This can be attributed to a quantum confinement effect in nanosize particles.

In nanoparticle semiconductors, quantum size confinement plays an important role in determining their electronic and optical properties. This effect becomes significant, particularly when the particle size is comparable to or smaller than the Bohr exciton radius. The Bohr diameter of ZnS is approximately 5 nm.[39] In our samples, depending upon the deposition time, the nanocrystallite size ranged from 3.0 to 4.7 nm, and the absorbance edges were observed in the UV region, approximately (3.75−3.65 eV). With consideration of the absence of ZnO ($E_{g,bulk} = 3.2$ eV) species in the films that have been confirmed by XPS and ATR-FTIR analyses, the observed blue shift in the absorption edge of these films compared with bulk ZnS ($E_{g,bulk} = 3.6$ eV) is attributed to the quantum confinement effect in ZnS:Mn nanocrystallites.

Fluorescence (FL) Spectra. Figure 11a shows the room-temperature fluorescence (FL) emission spectra of uncoated quartz slide as a blank as well as that of undoped and Mn-doped ZnS thin films grown on quartz substrates. ZnS:Mn thin film was prepared from a solution with Mn/Zn molar ratio of 4 at 80 °C. The excitation wavelength was 320 nm. It was found that the FL spectrum of the undoped ZnS film shows only one broad emission band at about 450 nm, which could be assigned to the radiative recombination involving defect states in the ZnS nanocrystalites.[5] The FL spectrum of the ZnS:Mn film consists of three characteristic bands, two narrow bands at ∼340 and ∼590 nm and one broadband over 370−450 nm range. However, a multiple Gaussian fit shown in Figure 11b, indicates four Gaussian bands centered at approximately 342, 384, 442, and 592 nm. The Gaussian curve fits well with the experimental curve, confirming the presence of four emission bands in the spectrum. The emission band at 442 nm was also observed in undoped ZnS film. The narrow UV emission peak at 342 nm corresponding to near-band-edge emission originates from the recombination of free excitons of ZnS. The emission bands centered at 384 and 442 nm should be assigned to stoichiometric vacancies (defect states) or interstitial impurities, possibly at the surface in the ZnS film.[40−43] The third emission band centered at 592 nm was assigned to $^4T_1 \rightarrow {}^6A_1$ transition within the 3d shell of Mn^{2+}.[4] Mixing between the s−p electrons of the host ZnS and the d electrons of Mn^{2+} occur when Mn^{2+} ions are incorporated into the ZnS lattice and substitute for the host cation sites. This partially allows the forbidden transition of $^4T_1 \rightarrow {}^6A_1$, resulting in the characteristic emission of Mn^{2+}.[4]

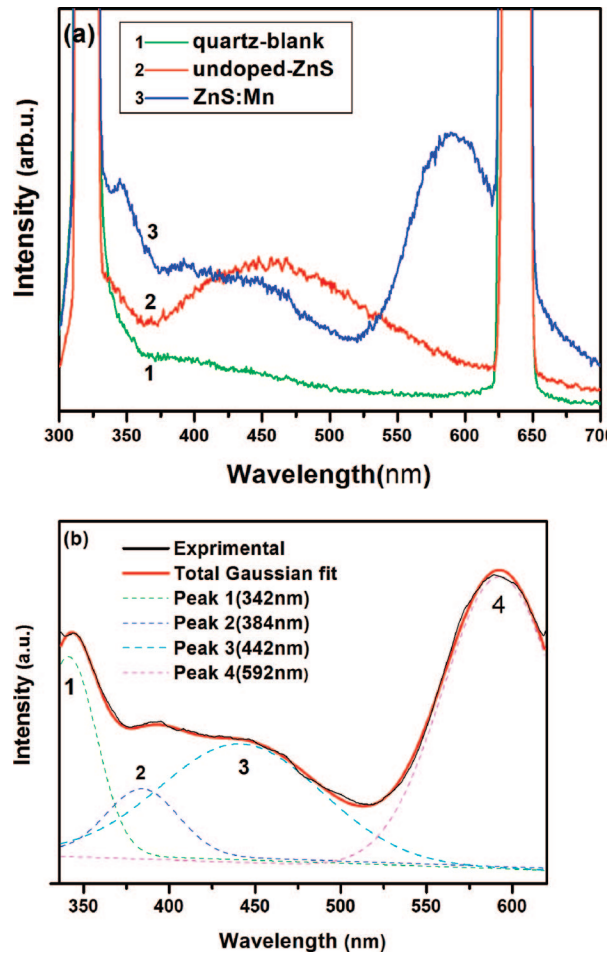

Figure 11. Fluorescence spectrum of the uncoated quartz (blank), ZnS, and ZnS:Mn films deposited on quartz substrates from a precursor solution with a Mn^{2+}/Zn^{2+} molar ratio of 4 at 80 °C for 4 h.

There are many reports on the origin of the blue emission band of ZnS upon ultraviolet irradiation. Kasai and Otomo[44] measured the electron paramagnetic resonance spectra (EPR) of a self-activated bulk sample and reported the existence of fluorescence centers of Zn^{2+} vacancies at the $g > 2$ region and S^{2-} vacancies at the $g < 2$ region, both emitting in the blue region. Becker et al.[45] examined the fluorescence of ZnS nanoparticles prepared using a colloidal method. They

(38) Elshabini-Raid, A. A. R.; Barlow, F. D. *Thin Film Technology Handbook*; McGraw-Hill: New York, 1998; pp 4−61.
(39) Rossetti, R.; Hull, R.; Gibson, J. M.; Brus, L. E. *J. Chem. Phys.* **1985**, *82*, 552.
(40) Bol, A. A.; Meijerink, A. *Phys. Rev. B* **1998**, *58*, 997.
(41) Kar, S.; Chaudhuri, S. *J. Phys.Chem. B* **2005**, *109*, 3298.
(42) Hu, P. A.; Liu, Y. Q.; Fu, L.; Cao, L. C.; Zhu, D. B. *J. Phys. Chem. B* **2004**, *108*, 936.
(43) Denzler, D.; Olschewski, M.; Sattler, K. *J. Appl. Lett.* **1998**, *84*, 2841.
(44) Kasai, P. H.; Otomo, Y. *J. Chem. Phys.* **1962**, *37*, 1263.
(45) Becker, W. G.; Bard, A. J. *J. Phys. Chem.* **1983**, *87*, 4888.

concluded that S^{2-} vacancies to be the origin of fluorescence at 428 nm. Uchida[46] studied fluorescence properties of bulk samples in correlation with the off-stoichiometry of Zn and S. He concluded that both excess Zn^{2+} and S^{2-} samples emit at ~450 nm after excitation with UV irradiation. The bulk sample made by Uchida emitted at 450 nm, whereas our nanocrystalline samples emitted at 428 nm. It is reasonable to assume that the emission from nanocrystallites has a blue shift because of quantum confinement effect.

It is well-known that Mn^{2+} can substitute for Zn^{2+} ions in the ZnS crystal lattice because of their close ionic radii (0.80 and 0.83 Å for Mn^{2+} and Zn^{2+}, respectively). The photoluminescence emission band at approximately 590 nm (yellowish orange) is a characteristic emission of Mn^{2+} ions in ZnS crystals.[47−49] Kennedy et al.[50] stated that there are two types of Mn in ZnS:Mn nanocrystallites (mean diameter of 3.5 nm). One is located inside the crystal or very close to another Mn. The other type of Mn is located at or near the surface. The latter shows the unusual fluorescence of interest.

Sooklal et al.[51] reported that Mn^{2+} incorporated into the ZnS lattice led to Mn^{2+}-based orange emission while ZnS with surface-bound Mn^{2+} yielded ultraviolet emission. In Figure 11a, no peak maximum was observed at 342 nm in an undoped ZnS film, unlike in the FL spectrum of the Mn-doped ZnS film. In the FL spectra of undoped ZnS and uncoated quartz as a blank, only a tail at about 340−360 nm is observed that is due to beam. Therefore, the observed peak at 342 nm must correspond to Mn bounded to the surface of the ZnS crystal lattice. So, the Mn^{2+} ions in our samples, besides being incorporated into the host ZnS nanocrystals (emission band at 590 nm), must also be surface-bounded to ZnS film (emission band at 342 nm). The SIMS analysis also confirmed the presence of Mn on the surface of the film.

Deposition Time Effect on FL Intensity. Figure 12 shows the fluorescence excitation and emission spectra of ZnS:Mn films prepared in different deposition times at 80 °C. The photoluminescence emission band at approximately 590 nm (2.1 eV; yellowish orange) is the characteristic emission of Mn^{2+} ions in ZnS crystals, which can be attributed to $^4T_1$ (excited) → $^6A_1$ (ground) transition of the Mn^{2+} ions in T_d symmetry.[48,49] Emission occurs through energy transfer from the excited state of the ZnS host lattice to the d electrons of Mn^{2+}. The absorption band in the excitation spectrum is due to the band-to-band transition of ZnS. Photoluminescence excitation (PLE) spectra corresponding to 590 nm emissions for ZnS:Mn films exhibit maxima at about 335 nm corresponding to the band gap excitation of host ZnS nanocrystals. This result clearly suggests that the emission at 590 nm (2.1 eV) arise from Mn^{2+} ions being incorporated into the ZnS nanocrystals and not from Mn^{2+} ions of MnS nanocrystals

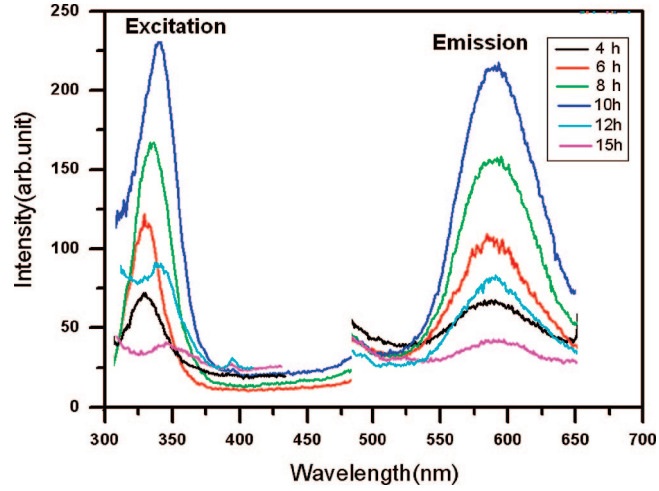

Figure 12. Excitation and emission bands of ZnS:Mn films prepared using a precursor solution with a Mn^{2+}/Zn^{2+} molar ratio of 4 at 80 °C as a function of the deposition time.

(It is important to note that the Mn^{2+} ions in MnS nanocrystals have two emission peaks at 1.66 and 1.8 eV).[52] Therefore, the presence of Mn^{2+} emission at 590 nm following excitation into the absorption band of ZnS indicates that Mn^{2+} ions occupy Zn^{2+} sites. The deposition time-dependent increase in orange emission can be explained as follows. It is known that there are randomly distributed defect centers in the nanocrystallites at the early stage of deposition.[53] Therefore, the fluorescence efficiency of Mn^{2+} inside the crystal is low because the excitation energies are transferred to the defect centers in the vicinity of Mn^{2+} ions. These defect centers will be occupied by Mn^{2+} ions, and their number in the crystal will decrease with time. Therefore, the crystallinity of the ZnS lattice and the distribution of Mn^{2+} ions in the ZnS crystal lattice improve with time, resulting in an increase in fluorescence intensity. The XRD pattern already confirmed the increment of ZnS:Mn film crystallinity with increasing deposition time (see Figure 5b).

In Figure 12, when the deposition time decreases, the excitation peaks shift slightly toward the blue (higher energy). The blue shift of the excitation peaks was interpreted as being due to an increase in the $^4T_1$ and $^6A_1$ states in the Mn T_d configuration, which was attributed to the quantum confinement effects due to a decrease in the nanocrystallite size of the films, as indicated in Table 2. However, the blue shift of the emission peaks are not attributed to the quantum confinement effects, because in nanoparticles, when the emission arises from a defect or a luminescence center such as Mn^{2+} or Eu^{3+}, the emission energies of these transitions are not size-dependent.[54] The blue shift of the emission peaks was interpreted as being due to a decrease in the $^4T_1$ and $^6A_1$ states in Mn T_d configuration (see Figure S-3, b → a, in the Supporting Information). A decrease in the $^4T_1$ and $^6A_1$ states in Mn is related to decreasing doping level of Mn in the ZnS lattice, as a result of decreasing deposition time.

(46) Uchida, I. *J. Phys. Soc. Jpn.* **1964**, *19*, 670.
(47) Angshuman, N.; Sameer, S.; Nagamani, A. S. *Chem. Mater.* **2007**, *19*, 3252.
(48) Gan, L. M.; Liu, B.; Chew, C. H.; Xu, S. J.; Chua, S. J.; Loy, G. L.; Xu, G. Q. *Langmuir* **1997**, *13*, 6427.
(49) Yu, I.; Isobe, T.; Senna, M. *J. Phys. Chem. Solids* **1996**, *57*, 373.
(50) Kennedy, T. A.; Glaser, E. R.; Klein, P. B.; Bhargava, R. N. *Phys. Rev. B* **1995**, *52*, R14356.
(51) Sooklal, K.; Cullum, B. S.; Angel, S. M.; Murphy, C. J. *J. Phys. Chem.* **1996**, *100*, 4551.
(52) Fan, D. B.; Yang, X. D.; Wang, H.; Zhang, Y. C.; Yan, H. *Physica B* **2003**, *337*, 165.
(53) Murase, N.; Jagannathan, R.; Kanematsu, Y.; Watanabe, M.; Kurita, A.; Hirata, K.; Yazawa, T.; Kushida, T. *J. Phys. Chem. B* **1999**, *103*, 754.
(54) Chen, W.; Bovin, J. P.; Joly, A. G.; Wang, S.; Su, F.; Li, G. *J. Phys. Chem. B* **2004**, *108*, 11927.

The changes in the excitation peak positions (Figure 12) match well with the absorption edge of the transmission spectra and band gap energy of the films, as shown in Figure 9 and Table 2, respectively.

As shown in Table 2, the excitation peaks appeared at higher energy related to their band gap values. This is reasonable and is related to the excitation of electrons from the ground state of the valence band to vibration excited states in the conduction band, as shown in Figure S-3 (see the Supporting Information).

For example, the excitation peak and the band gap energy of the film with 6 h deposition time were observed at 330.6 nm (3.75 eV) and 337 nm (3.68 eV), respectively.

Temperature Effect on FL Spectra. The homogeneous distribution of Mn^{2+} ions in a ZnS crystal lattice is quite important for efficient luminescence.[48,49,54−57] When there is an inhomogeneous distribution of Mn^{2+} ions, local Mn^{2+}−Mn^{2+} pairs or clusters form in the ZnS crystals, which interact and lead to nonradiative relaxation under excitation.[57,58] This results in a lower luminescence efficiency. In addition, the photoluminescence (PL) spectrum of semiconductors is closely related to the crystalline quality. The donor and acceptor populations, trapping and recombination centers, stress and dislocations, etc., can have a significant influence on the PL spectra because the electronic transitions are quite sensitive to the defect levels in the forbidden band gap of the material.[59]

During the CBD process, ZnS forms the main phase, whereas Mn^{2+} is present as an impurity and can be incorporated gradually into the ZnS crystal lattice, depending on the process conditions. With increasing chemical bath temperature and deposition time, it seems that Mn^{2+} can more effectively diffuse and incorporate into the ZnS lattice. Higher deposition temperatures also promote a higher degree of crystallinity, thereby eliminating crystal defects. Therefore, the fluorescence usually increases with increasing process temperature over a suitable temperature range. As shown in Figure 13, at 50 and 60 °C, the ZnS:Mn films did not show any significant fluorescence because the crystallinity was low and Mn^{2+} was not incorporated effectively into the ZnS crystal lattice, probably existing near the ZnS crystal surfaces. At 70 and 80 °C, Mn^{2+}can effectively incorporate into the ZnS crystal lattice because the nanocrystals grow faster at 70 and 80 °C than at 50 °C, implying a significant increase in the movement of Mn^{2+} and Zn^{2+} ions and rearrangements on the surface and inside of the ZnS crystal lattice. This is beneficial to the spatial isolation or homogenization of Mn^{2+} ions as well as to the elimination of crystal defects. As a result, the fluorescence intensity is higher for ZnS:Mn films prepared at 70−80 °C.

Quantum Size Effect on FL Spectra. An improvement in the quantum size effect of a ZnS:Mn^{2+} phosphor, i.e., the

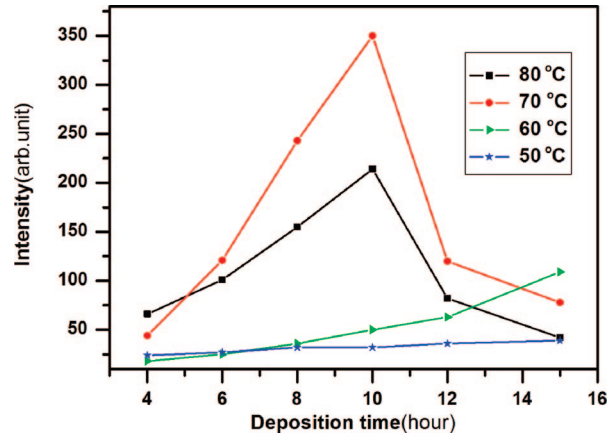

Figure 13. Effect of temperature on the fluorescence intensity of ZnS:Mn films prepared from precursor solutions with a Mn^{2+}/Zn^{2+} molar ratio of 4 as a function of the deposition time.

luminescence efficiency of the blue-shifted band in nanocrystallites, is frequently observed in crystals with a mean size <5 nm.[4,48,49,60] The measured Mn concentration by ICP-AES in our prepared films during 10 h deposition time at 70 and 80 °C was 0.57 and 0.94 at % (relative to Zn), respectively. Interestingly, despite the lower Mn amount in the film prepared at 70 °C, its fluorescence intensity was stronger than that of the film prepared at 80 °C. This increase in the fluorescence emission intensity is attributed to quantum size effects because the nanocrystalline size of ZnS:Mn films prepared at 70 °C is smaller than that of at 80 °C and both are less than 5 nm. As mentioned previously, particles with diameters less than or comparable to the Bohr diameter of ZnS (5 nm) show strongly quantum confinement effect. Increasing FL intensity by the quantum size effect can be explained as follows; Bhargava et al.[4] suggested that the transition between $^4T_1$ and $^6A_1$ in nanocrystalline Mn-doped ZnS is enhanced because of quantum confinement effects. They reported that the radiative transition is approximately 5 orders of magnitude faster in the nanoparticles than in the bulk. Bhargava and/or his co-workers[4,61] suggested that a strong hybridization of the s−p states of the ZnS host and d states of the Mn^{2+} impurity should occur with decreasing particle size. This hybridization results in more rapid energy transfer between the ZnS host and Mn^{2+} impurity. Because of this rapid energy transfer, the radiative recombination in the Mn^{2+} impurity, which competes with nonradiative decay at the ZnS surface, becomes more efficient. This results in an increase in quantum efficiency.

Mn^{2+} Concentration Effect on FL Spectra. Concentration quenching effect on the photoluminescence intensity of Mn^{2+}-doped ZnS nanocrystallites has been observed in many studies. The existence of an optimum Mn^{2+} doping concentration has been attributed to the presence and interaction of Mn^{2+}−Mn^{2+} ion pairs or clusters with increasing Mn^{2+} concentration.[57] The process involves the resonant transfer of electronic excitation energy from one activated ion (Mn^{2+})

(55) Hunter, A.; Kitai, A. H. *J. Appl. Phys.* **1987**, *62*, 4244.
(56) Bin, X. I.; Wuled, L.; Kikuo, O. *Chem. Mater.* **2002**, *14*, 4969.
(57) Yu, I.; Senna, M. *Appl. Phys. Lett.* **1995**, *66*, 23.
(58) Bessergenev, V. G.; Belyi, V. I.; Rastorguev, A. A.; Ivanova, E. N.; Kovalevskaya, Yu A.; Larionov, V. G.; Zemskova, S. M.; Chirichenko, V. N.; Nadolinnyi, V. A.; Gromilov, S. A. *Thin Solid Films* **1996**, *279*, 135.
(59) Lozada-Morales, R.; Zelaya-Angel, O.; Torres-Delgado, G. *Appl. Surf. Sci.* **2001**, *175*, 562.
(60) Suyver, J. F.; Wuister, S. F.; Kelly, J. J.; Meijerink, A. *Nano Lett.* **2001**, *1*, 429.
(61) Bhargava, R. N. *J. Lumin.* **1996**, *70*, 85.

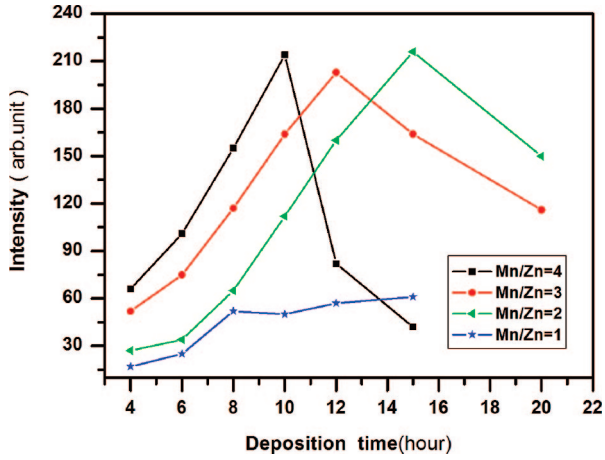

Figure 14. Effects of the doping level on the FL intensity of films as a function of the deposition time at 80 °C.

to another, and to a quenching site (e.g., a defect) after a number of energy transfer steps.[62]

Sooklal et al.[51] reported an optimal Mn^{2+} concentration of 2%. Khosravi et al.[6] observed a maximum luminescence at a doping concentration of 0.12 wt %. Leeb et al.[63] and Qi and Chong[64] reported an optimal Mn^{2+} concentration of 1 and 1.5%, respectively.

The concentration quenching effect was also observed in our samples. Figure 14 and Table 2 shows the effects of the Mn doping level on the FL intensity of ZnS:Mn films as a function of the deposition time at 80 °C. As shown in this figure, for all doping levels (except $Mn^{2+}/Zn^{2+} = 1$), the FL intensity increased gradually with increasing deposition time, reaching a maximum at some point. With further increase in deposition time, the FL intensity decreased noticeably, showing the concentration quenching effect. For the films prepared in the precursor solution with a Mn^{2+}/Zn^{2+} molar ratio of 1, which show very low emission intensity, it could be assumed that Mn^{2+} was either not activated or could not be incorporated effectively into the ZnS lattice because of insufficient Mn^{2+} in the precursor solution. On the other hand, with increasing Mn^{2+} concentration in the precursor solution, Mn^{2+} can more effectively diffuse into the ZnS, and as a result, the prepared films at higher doping levels have strong emission intensity (Figure 14, $Mn^{2+}/Zn^{2+} = 2-4$). Defect centers act as quenching sites or factors in a crystal lattice.[62] When the doping level increases, more numbers of empty sites (defects) are occupied by Mn^{2+} substitution. Therefore, the number of quenching sites (defects) decreases and FL intensity increases. Indeed, a higher Mn^{2+} concentration promotes a higher degree of crystallinity by eliminating crystal defects and increasing the fluorescence intensity.

As shown in Figure 14, when the doping level in the precursor solution was decreased from 4 to 2, the maximum emission intensity and quenching concentration effect shifted to a longer deposition time, from 10 to 15 h. The maximum emission intensity did not change. The Mn/Zn atomic percent ratios for the points which have the maximum emission intensity were measured by ICP-AES and listed in Table 3. In Table 3, the obtained Mn/Zn ratios and their nanocrystallite sizes are close to each other, suggesting that the prepared ZnS films from the precursor solutions with different doping levels reach a saturation state but at different times. The strongest emission intensities are observed in these states, and after that, with increasing deposition time, more Mn^{2+} diffuse into the crystal lattice or surface of ZnS lattice, and thus a quenching effect appears. The shift in the quenching effect to a longer deposition time with decreasing doping level can be explained as follows. The diffusion rate of Mn^{2+} ions into the empty sites (defects) of ZnS crystal lattice decreases with decreasing Mn^{2+} concentration in the precursor solution. Indeed, the formation of a saturation state takes places at a longer deposition time. Therefore, the maximum emission intensity and quenching effect shifts to a longer deposition time with decreasing doping level in the precursor solution.

Table 3. Crystallite Size, Mn/Zn Ratios Incorporated and Used in the Preparation of the Films with Maximum FL Intensity

deposition time (h)	Mn/Zn molar ratios used in the precursor solutions	Mn/Zn % ratio in films, measured by ICP-AES	nanocrystal size (nm) estimated using Sherrer eq
10	4	0.94	4.2
12	3	1.07	4.5
15	2	1.20	4.7

Conclusions

In this study, ZnS:Mn thin films were prepared using a chemical bath deposition method with Na_2EDTA as the complexing agent for zinc ions and TAA as the S^{2-} ions source in a aqueous solution at temperatures ranging from 50 to 80 °C. The film thickness was controlled by the deposition temperature and time. The prepared films were highly transparent (>80%) in the visible region. The steep absorption edge of the films and FE-SEM images demonstrated a dense and uniform surface that was free of pits or pinholes with a narrow grain size distribution. The FL intensity of the films is strongly dependent on the temperature, deposition time, doping level, and exhibited a quantum size effect. It was found that the Mn^{2+} $^4T_1 \rightarrow {}^6A_1$ emission intensity of the ZnS:Mn thin films increased significantly with increasing Mn^{2+} concentration, and showed a maximum when the Mn^{2+} to Zn^{2+} molar ratio was 4 in the precursor solutions. The highest concentration of Mn doped into ZnS nanocrystalline thin films was found to be 1.5% (relative to Zn^{2+}). The FL data also showed that Mn^{2+} ions were incorporated into the ZnS host lattice and bound to the surface of the ZnS nanocrystals. XRD revealed the films to consist of small ZnS: Mn grains ranging in size from 3.0 to 4.7 nm. In addition, the film crystallinity increased with increasing temperature and deposition time. Since the prepared ZnS:Mn films show strong emission and are highly transparent in the visible range, they can be used to fabricate flat panel displays in phosphor applications.

(62) Blasse, G.; Grabmaier, B. C. *Luminescent Materials*; Springer-Verlag: Berlin, 1994.
(63) Leeb, J.; Gebhardt, V.; Mu1ller, G.; Haarer, D.; Su, D.; Giersig, M.; McMahon, G.; Spanhel, L. *J. Phys. Chem. B* **1999**, *103*, 7839.
(64) Qi, X.; Chong, X. *Appl. Surf. Sci.* **2008**, *254*, 6432.

Acknowledgment. The authors thank Mr. Chi-Wan Kim for the thickness measurements and all other graduate students in the Nano-Information Materials Laboratory in Pusan National University, Korea, for their cooperation. This work was supported for 2 years by the Pusan National University Research Grant.

Supporting Information Available: Experimental condition of the F-4500 FL spectrophotometer; EDX data for uncoated polycrystalline Si substrate; EDX spectra of uncoated polycrystalline Si substrate and ZnS:Mn thin films deposited on Si substrate and prepared from the precursor solution with Mn/Zn molar ratio of 4 at 80 °C; energy-level diagram of ZnS:Mn nanoparticles (PDF). This material is available free of charge via the Internet at http://pubs.acs.org.

CM803329W